UNIVERSITY OF
LATVIA

Summary of
Doctoral Thesis

Viktors Romaņuks

CHEMICAL MODIFICATION OF RECOMBINANT SPIDER SILK PROTEINS

Riga 2025

UNIVERSITY OF
LATVIA

FACULTY OF MEDICINE
AND LIFE SCIENCES

Viktors Romaņuks

CHEMICAL MODIFICATION OF RECOMBINANT SPIDER SILK PROTEINS

SUMMARY OF DOCTORAL THESIS

Submitted for the degree of PhD of Natural sciences
Field of Chemistry

Subfield: Organic chemistry

Riga 2025

The doctoral thesis was carried out: at the Latvian Institute of Organic Synthesis, from 2019 to 2025.

The thesis contains the introduction, 3 chapters, reference list, 3 appendices.

Form of the thesis: dissertation in chemistry, subfield of organic chemistry.

Supervisor: Dr. Chem. **Gints Šmits**.

Reviewers:
1) Dr. chem. Antons Sizovs (Latvian Institute of Organic Synthesis);
2) Dr. pharm. Edijs Vāvers (University of Tartu);
3) Dr. sc. ing. Dagnija Loča (Baltic Biomaterials Centre of Excellence).

The thesis will be defended at the public session of the Doctoral Committee of Chemical Science, University of Latvia, at 12.00 on December 19. 2025.

The thesis is available at the Library of the University of Latvia, Riga Raiņa blvd. 19.

Promotion Council in
the Field of Chemistry,
University of Latvia
Chairman _____ / Prof. Dr. chem. **Edgars Sūna** /
(signature)

Secretary _____ / Assoc. Prof. Dr. chem. **Vita Rudoviča** /
(signature)

ISBN 978-9934-36-465-5
ISBN 978-9934-36-466-2 (PDF)

ANNOTATION

Chemical Modification of Recombinant Spider Silk Proteins. Romaņuks, V. Supervisor: Dr. Chem. Šmits, G. Doctoral Thesis, 88 pages, 61 figures, 9 tables, 233 references, and 3 appendices. Written in Latvian.

The thesis is devoted to the development of new methods for the efficient production of recombinant spider silk proteins and their processing into biomaterials.

The scientific novelty of the developed methods lies in an original approach – introducing a cysteine residue into the C-terminal domain of spider silk proteins, which enables specific and efficient thiol–maleimide conjugation between minispidroins and PEG containing maleimide groups. This method significantly simplifies the production of recombinant spider silk, reduces the need to express full-length spidroins, and allows tuning of material properties by varying the parameters and reagents of the bioconjugation process.

Within the scope of the work, the expression, purification, and bioconjugation of spidroins were optimized, the suitability of the obtained bioconjugates for fiber spinning was evaluated, and the physical properties of the resulting fibers were analyzed. The obtained fibers exhibit physical properties comparable to, or in some cases surpassing, those produced from higher molecular weight proteins.

Thus, this work provides a significant contribution to materials science, with an emphasis on the development of biodegradable materials for biomedical and tissue engineering applications.

Keywords: bioconjugation, spidroins, artificial spider silk, PEG, fibers.

TABLE OF CONTENTS

LIST OF ABBREVIATION

Cys	Cysteine
CT	C-terminal domain
DCM	Dichloromethane
DTT	1,4-Dimercapto-2,3-butanediol
EtOAc	Ethyl acetate
FlSp	Flagelliform silk spidroins
IPTG	Isopropyl-β-D-1-thiogalactopyranoside
LB	*Luria-Bertani* medium
Mal	Maleimide
MaSp	Major ampullate silk spidroins
NHS	*N*-hydroxysuccinimide
NT	*N*-terminal domain
OD_{600}	Optical density at 600 nm wavelength
PBS	Phosphate-buffered solution
PEG	Polyethylene glycol
SCM	Succinimide
SDS-PAGE	Sodium dodecyl sulfate–polyacrylamide gel electrophoresis
TCEP	Tris(2-carboxyethyl)phosphine
THF	Tetrahydrofuran

GENERAL CHARACTERISTICS OF THE WORK

Topicality of the Research

Spider silk is considered one of the most durable natural materials and has attracted the attention of researchers in both academia and industry for several decades. Its strength, elasticity, low density, and other mechanical parameters have proven to be superior even to those of one of the toughest synthetic polymers – Kevlar. In addition, spider silk is both biocompatible and biodegradable, making it an attractive material not only from a materials science perspective but also for applications in cosmetics and medicine.

In nature, spiders are capable of producing up to seven different types of silk for web construction (Fig. 1).

Major ampullate (MA) silk is used to construct the main framework of the web, while flagelliform (FlSp) silk is employed in the formation of the capture spiral. Aggregate silk provides a sticky coating on the capture spiral, whereas minor ampullate (Mi) silk is used to build auxiliary spirals and reinforce the web structure. Pyriform silk is applied to create attachment discs on surfaces. Aciniform silk is utilized for prey wrapping and for forming protective egg case layers, while cylindriform silk is specifically used in the construction of the egg sac cover. [1]

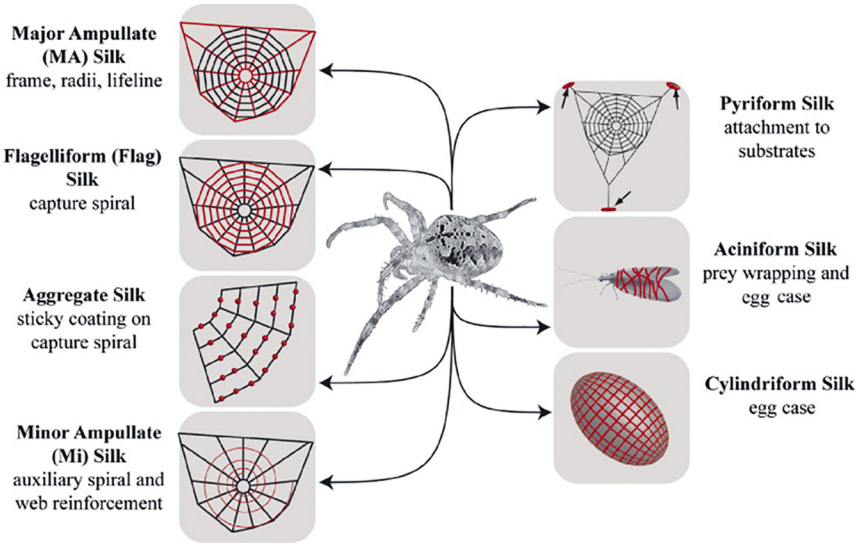

Fig. 1. **Schematic representation of the seven types of spider silk.[1]**

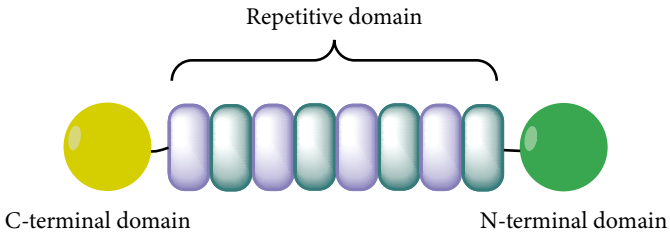

Fig. 2. **Schematic structure of a spidroin.**

The global demand for spider silk is estimated in the hundreds of tons annually, with a market value exceeding USD 2 billion, and this demand continues to grow each year. [2] Nevertheless, large-scale production of spider silk and its constituent proteins (spidroins) still presents considerable challenges. The primary reason is the cannibalistic and territorial lifestyle of spiders, which prevents direct industrial-scale harvesting of silk from spiders. This limitation has stimulated the development of alternative biotechnological approaches for large-scale production of recombinant spidroins. One of the most widely used methods is the expression of recombinant proteins in *Escherichia coli*. [3] More rarely, recombinant spidroins are obtained from yeast [4], plants [5], animals, or animal cell cultures. [6, 7] Materials produced in this way are commonly referred to as recombinant spider silk.

Natural spider silk consists of three fundamental building blocks (Fig. 2):

- **C-terminal domain (CT):** enhances spidroin solubility and promotes fiber formation within the spider's gland.
- **N-terminal domain (NT):** dimerizes in response to pH and environmental changes, thereby facilitating fiber assembly.
- **Repetitive domain:** accounts for approximately 90% of all spidroin amino acids and is primarily responsible for the physical properties of silk.

For example, major ampullate silk (MaSp) is predominantly composed of glycine and alanine residues in the repetitive domain, which confer strength and rigidity to the silk, whereas flagelliform silk (FlSp) is enriched in glycine and proline residues, resulting in significantly greater elasticity. [8]

To increase the efficiency of spidroin production, particularly in bacterial systems, minispidroins are engineered in which the repetitive domain is considerably shorter than in full-length spidroins. These minispidroins can subsequently be bioconjugated with polymers or other compounds. This approach enables direct modification of the protein structure, ultimately allowing improvements in protein pharmacokinetics, solubility, conjugate stability, and physical properties. Such modifications can be achieved through chemical strategies, for example using carbodiimides or activated esters, as well as by employing the increasingly popular methods of "click chemistry." [9] Polyethylene glycol (PEG) is one of the most widely used polymers in protein bioconjugation. Currently, more than

20 PEG–protein conjugates are available on the market. These bioconjugates have broad applications, ranging from the prevention of chemotherapy-induced neutropenia to the treatment of rare inherited metabolic disorders. Conjugated coagulation factors (e.g., *Adynovate* [10]) are applied in hemophilia therapy, whereas conjugated antibody fragments, such as certolizumab pegol (*Cimzia* [11]), are used in the treatment of autoimmune diseases including Crohn's disease and rheumatoid arthritis. [12]

Aim and Objectives of the Study

The aim of this doctoral thesis is to develop a new and efficient method for the production of recombinant spider silk by employing bioconjugation of silk-forming minispidroins with PEG, combined with biomimetic spinning.

To achieve this aim, the following objectives were set:

1. To investigate and optimize the reaction conditions for spidroin bioconjugation;
2. To evaluate the spinning efficiency of different bioconjugates;
3. To analyze the physical properties of the obtained fibers;
4. Protein production scale-up.

Scientific Novelty and Main Results

As a result of this work, a method was developed and optimized for the production of minispidroins in a bioreactor, yielding protein amounts more than an order of magnitude higher than those attainable in flask cultures. A procedure for minispidroin bioconjugation with polyethylene glycol was established and optimized, achieving substitution levels exceeding 70%. The resulting PEG–minispidroin conjugates were spun in a biomimetic manner, producing fibers whose physical properties were comparable to, and in some cases surpassed, those of other artificial fibers based on similar proteins.

Validation of the Dissertation Results

Scientific Publications

- Romaņuks, V., Fridmanis, J., Schmuck, B., A. L. Bula A. L., Lends, A., Senkane, K., Leitis, G., Gaidukovs, S., Smits, K., Rising, A., Smits, G., Jaudzems, K., Biomimetic Spider Silk by Crosslinking and Functionalization with Multiarm Polyethylene Glycol. *Adv. Funct. Mater.* **2024**, 2409487.

Patents

- Jaudzems, K.; Romaņuks, V.; Frīdmanis, J.; Bula, A., L.; Šmits, G. Chemically modified engineered spider silk proteins. WO2023227926A1, 30.11.2023

Conference Abstracts

- Romaņuks, V. Artificial spider silk by crosslinking and functionalization with multi-arm polyethylene glycol. *8th China-Europe Symposium on Biomaterials in Regenerative Medicine*, 15–18 september, **2024,** Nuremberg, Germany. CESB 2024 Book of Abstracts, pp. 143–144.
- Romaņuks, V. Biomimetic Spinning of Crosslinked and Functionalized Spider-Silk Proteins with Multiarm Polyethylene Glycol. *7th International Conference on Chemistry*, 11–12 november, **2024**, Barcelona, Spain.
- Romaņuks, V. Ķīmiski modificēts mākslīgs zirnekļa zīds. *Latvijas materiālu pētīšanas biedrības 31. kongress*, 27 march, **2025**, Riga, Latvia.

MAIN RESULTS OF THE DISSERTATION

1. Spidroin Production

The first objective of this work was the production of spider silk proteins (spidroins) for further studies. For this purpose, we selected the most commonly used approach – heterologous expression (synthesis) of spidroins in bacteria. Natural spidroins are large biomolecules with molecular weights reaching up to 350 kDa. [1] Expression of such large spidroins in bacterial systems is inefficient, as it leads to plasmid instability and low protein solubility. For example, a protein of 46 kDa containing a single repetitive domain exhibits solubility of 565 mg/mL, whereas its longer variant of 104 kDa with four repetitive domains shows solubility reduced to only 134 mg/mL. [13] Consequently, protein expression yields are also lower; in the aforementioned case, the obtained yields were 254 mg/L and 89 mg/L, respectively. [14]

To increase expression yields of spidroins and to facilitate subsequent bioconjugation with PEG, we chose to express minispidroins, in which the repetitive domain is significantly shorter than in natural spidroins. Furthermore, the C-terminal domain was replaced with a cysteine residue, enabling maleimide–thiol conjugation. This strategy allowed the formation of protein conjugates ranging from dimers to octamers, covalently linked via PEG. These conjugates subsequently dimerize through their N-terminal domains at low pH, thereby forming fibers.

The minispidroins obtained in this work (Fig. 3) contain the N-terminal domain of *N. clavipes* FlSp, which is highly soluble in water and dimerizes at pH ~5.5. [15–17] The repetitive domain was derived either from *N. clavipes* FlSp or from *E. Australis* major ampullate spidroin 1 (MaSp1). The F2M protein contains the above-mentioned N-terminal domain and two repetitive domains from *E. Australis*; F4M contains four repetitive domains; and F6M contains six repetitive domains. F2F, in turn, contains the same N-terminal domain and two repetitive domains from *N. Clavipes*.

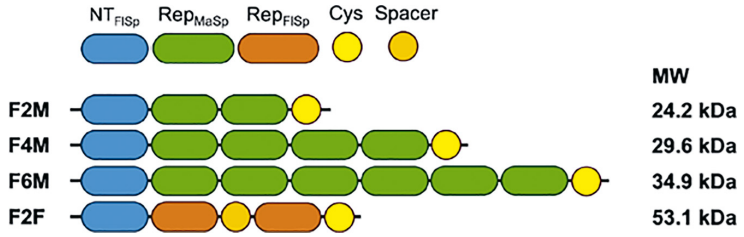

Fig. 3. **Structures of the spidroins used and the molecular weights of their monomers.**

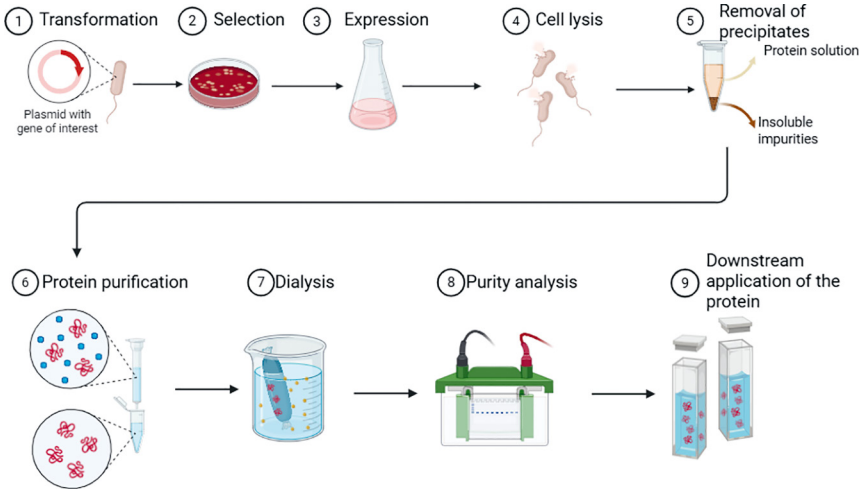

Fig. 4. **General scheme for protein production.**

Spidroins were obtained using the workflow shown in Fig. 4. In the first step, chemically competent *E. coli* cells were transformed with a plasmid – a small DNA construct containing both the coding sequence of the target protein and an antibiotic resistance gene. The cells were subsequently plated on 1/100 LB agar plates supplemented with 50 µg/mL kanamycin and incubated overnight at 30 °C (Fig. 4, Step 2). A single colony was then inoculated into 50 mL of LB medium containing 50 µg/mL kanamycin and cultured overnight at 25 °C. The resulting overnight culture was further expanded into 1 L of LB medium, and OD_{600} was measured, which at this stage typically averaged around 0.01. The culture was transferred into 2.5 L Erlenmeyer flasks and incubated at 37 °C until OD600 reached ~0.6. Protein expression was induced with 0.05 mM IPTG while lowering the incubation temperature to 25 °C. After overnight expression, the cells were harvested by centrifugation at 7000 × g for 15 min at 4 °C (Fig. 4, Step 3).

Following cell lysis (Fig. 4, Step 4) and removal of insoluble material (Fig. 4, Step 5), proteins were purified by nickel affinity chromatography (Fig. 4, Step 6). Fractions containing the target protein were pooled and dialyzed to remove imidazole (Fig. 4, Step 7), and subsequently concentrated. Finally, the purity of the obtained proteins was verified by SDS–PAGE analysis (Fig. 4, Step 8). The expression yields of the recombinant proteins are summarized in Table 1.1.

From the obtained results, it can be concluded that all of these minispidroins exhibited relatively good expression levels, and the yields are consistent with literature values, which typically range from 10 to 300 mg/L. [8, 18, 19] Increasing the number of repetitive domains drastically reduced protein yield.

Table 1.1. **Efficiency of Minispidroin Production**

Minispidroin	Average protein yield, mg/L of cell culture
F2M	116.0±17.4
F4M	50.6±11.2
F6M	30.1±11.4
F2F	56.0±10.2

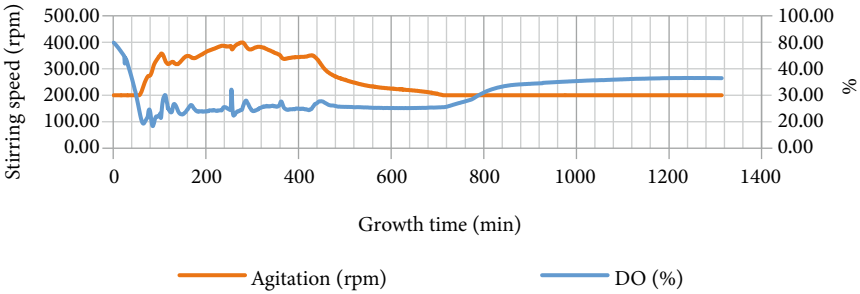

Fig. 5. **Changes in stirring speed and dissolved oxygen during bioreactor operation.**

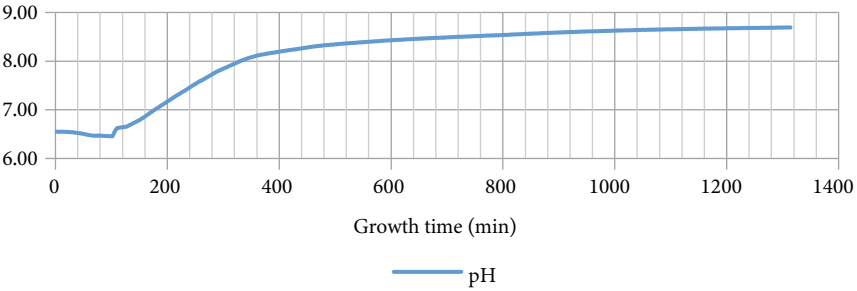

Fig. 6. **pH Changes During Bioreactor Operation.**

When comparing our results with those reported in the literature for bioreactor-based production – where researchers achieved yields an order of magnitude higher than for the same protein expressed in flasks [20], it can be inferred that protein yields in a bioreactor can indeed exceed flask yields by up to an order of magnitude. This is explained by the superior aeration, controlled pH, and continuous nutrient supply available in a bioreactor, all of which support more efficient bacterial growth. A successful transition from flask-based to bioreactor-based protein expression requires optimization of multiple parameters, including oxygen supply, pH regulation, nutrient feed, mixing rate, incubation temperature, and other factors, as well as an understanding of the intrinsic kinetics of the process.

In our initial experiment, we employed LB medium to produce FlSp protein; however, the primary aim of this experiment was to characterize the growth kinetics in the bioreactor.

From the obtained results, we concluded that without pH control the active bacterial growth phase lasts for approximately 450 minutes after inoculation, after which the medium becomes too alkaline to support further bacterial growth. This indicates that the first essential optimization step is pH regulation. Additionally, the observation that the maximum stirring speed was nearly reached suggests that a higher oxygen supply than the standard 1 L/min compressed air per 1 L of medium is required. From the first experiment, we obtained 50 mg of F2F protein per liter of culture medium, which is comparable to flask-based expression.

By modifying the culture conditions in accordance with literature reports [20, 21] – increasing aeration and stirring speed, removing glucose from the medium, and actively feeding the cells during growth – we obtained 413 g of wet cell mass from 2 liters of medium. Based on BugBuster analysis, the theoretical maximum for the target protein was estimated at 2.6 g/L of medium. After purification, 1.93 g/L of protein was recovered.

Since recombinant spider silk proteins denature at higher temperatures than most contaminating proteins, it is possible to selectively precipitate the majority of unwanted proteins while retaining the target protein in solution. For freshly obtained lysates, protein mixtures were subjected to heat treatment at 50 °C, 60 °C, and 70 °C for 15 minutes with continuous stirring. At the end of heating, the samples were rapidly cooled in an ice–water bath, centrifuged at 8000 × g, decanted, and analyzed by SDS–PAGE.

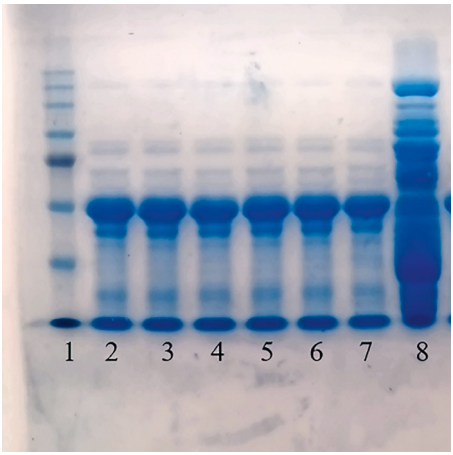

Fig. 7. **SDS–PAGE gel of samples after heat treatment. Lane 1 – molecular weight marker; lanes 2–7 – heat-treated sample at 50 °C; lane 8 – untreated material.**

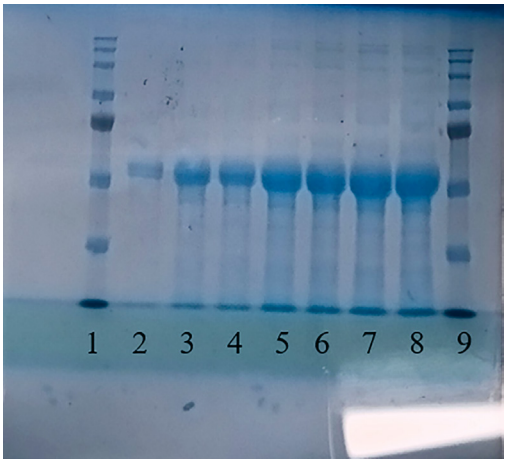

Fig. 8. **SDS–PAGE gel of samples after heat treatment at 60 °C.**

From the obtained results (Figs. 7 and 8), it can be seen that the protein can be recovered in a relatively pure form after heat treatment at 50 °C, and in sufficiently high purity (>80%) after treatment at 60 °C. At 70 °C, however, the sample partially coagulated, making further analysis impossible.

2. Optimization of Bioconjugation

The next step after protein production was bioconjugation (Fig. 9) and, accordingly, optimization of this reaction. Since the protein obtained in the previous steps typically existed in solution as a disulfide dimer **1**, it was first necessary to reduce it in order to generate the free thiol **2**, which could subsequently be conjugated to form the desired conjugate **3**. Classically, this reduction is carried out using water-soluble TCEP or DTT. Because the TCEP reduction method is easier to implement and the reagent itself is more stable during storage, we employed TCEP in subsequent experiments.

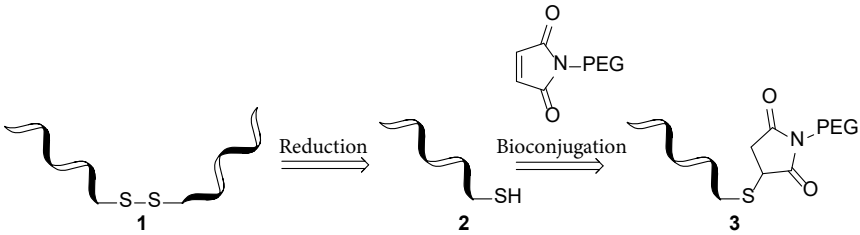

Fig. 9. **Bioconjugation of recombinant spider silk proteins with PEG.**

Table 2.1. **Comparison of Methods for Inhibition/Removal of Unreacted TCEP**

	2-arm PEG-Mal with azide inhibition	2-arm PEG-Mal with nickel affinity column
Unreacted protein	12 %	10 %
Monoconjugated	39 %	15 %
Diconjugated	44 %	75 %

All following reactions were performed in 20 mM sodium phosphate buffer containing 300 mM NaCl at pH 7.2. During optimization of the reduction step, the following parameters were examined: amount of reducing agent, duration of reduction, temperature, method for inhibiting the reducing agent, and the presence of additives. After reduction, the protein was conjugated with PEG at a fixed stoichiometry and analyzed by sodium dodecyl sulfate–polyacrylamide gel electrophoresis (SDS–PAGE).

In the course of the work, we optimized the following parameters: stoichiometry of reducing agent (10 eq., 20 eq., 30 eq., 50 eq., and 100 eq.), duration of reduction (16 h, 24 h, 48 h, and 72 h), and temperature (4 °C, 20 °C, and 37 °C). Inhibition of excess reducing agent was carried out using PEG azides. These azides are water-soluble and rapidly react with TCEP under mild conditions via a Staudinger-type mechanism, converting it into an oxidized, inactive form. [21] As an alternative, a nickel affinity column was employed to remove residual TCEP chromatographically.

After several optimization cycles, it was concluded that the most effective reduction conditions were as follows: 10 equivalents of TCEP, carried out at 4 °C for 24 hours. Excess TCEP was most efficiently removed from the reaction mixture using a nickel affinity column, while the presence of additives in the solution did not improve the efficiency of reduction. Increasing the amount of TCEP, the reduction time, or the temperature led to undesirable protein aggregation and subsequent precipitation. Compared with desalting chromatography, the use of PEG azides for inhibition of unreacted TCEP was not sufficiently effective, resulting in significantly lower yields of subsequent bioconjugation (Table 2.1).

After optimization of the reduction step, the next stage was to optimize the bioconjugation process. The following parameters were examined: reaction temperature (4 °C, 20 °C, and 37 °C), stoichiometry of reagents (ranging from 0.5 equivalents of protein per maleimide group (arm) to 3 equivalents of protein per arm), duration of the bioconjugation reaction (16 h or 24 h), and rate of protein addition (~1 mL/min). Bioconjugation was performed with the following PEGs: 2-arm PEG, which allows the formation of linear conjugates, and 4-arm or 8-arm PEG, which can potentially yield cross-linked conjugates.

After several optimization cycles, it was concluded that, similar to reduction, bioconjugation should be carried out at 4 °C. Reaction duration had only a minor effect on efficiency. The optimal stoichiometric ratio was approximately

1.2 equivalents of protein per arm, with gradual addition of the protein. As with the reduction step, prolonged reaction times at elevated temperatures led to protein aggregation and precipitation. Increasing the protein-to-arm ratio did not enhance substitution efficiency, whereas gradual protein addition resulted in higher conjugation yields compared to rapid addition.

From the obtained results (Table 2.2), it can be concluded that, on average, 50–70% of proteins were successfully conjugated with the polymer. Unfortunately, in none of the cases was it possible to achieve complete product conversion with full substitution.

One of the aims of this dissertation was to obtain spidroins covalently modified with lipophilic alkyl chains. Such modifications could potentially allow control of moisture content in the spun fibers – preventing them from either completely drying out or absorbing excessive amounts of water.

For this purpose, a heterobifunctional PEG **4** can be employed, in which one arm carries a succinimide or hydroxyl group, while the other three arms are maleimides (Fig. 10). The heterobifunctional polymer **4** may first be functionalized with a lipophilic moiety to form the intermediate **5**, which in the subsequent step can be conjugated with the free thiol group of protein **2**, yielding the corresponding conjugate **6**.

Initially, we tested the conjugation of Mal-PEG-OH with aliphatic carboxylic acids using the Steglich esterification method (Fig. 11).

Although the esterification reaction itself appeared to proceed successfully, we found that during purification – using either normal-phase or reversed-phase chromatography – product **9** underwent degradation due to cleavage of the maleimide double bond. Precipitation of the product also did not yield satisfactory results. Consequently, this method was not employed in further studies.

Table 2.2. **Summary of bioconjugation results**

	F2M-2 arm PEG	**F2M-4 arm PEG**	**F2M-8 arm PEG**	**F4M-2 arm PEG**	**F4M-4 arm PEG**	**F6M-2 arm PEG**	**F6M-4 arm PEG**	**F2F-2 arm PEG**	**F2F-4 arm PEG**	**F2F-8 arm PEG**
Unreacted protein	46 ± 17%	57 ± 3%	–	50 ± 7%	39 ± 9%	45 ± 9%	43 ± 6%	18 ± 5%	50 ± 7%	32 ± 7%
Monocon.	15 ± 8%	0%	0%	20 ± 4%	0%	23 ± 5%	9 ± 3%	50 ± 15%	6 ± 1%	0%
Dicon-jugated	39 ± 19%	13 ± 2%	9 ± 1%	30 ± 3%	24 ± 3%	32 ± 5%	22 ± 2%	32 ± 11%	20 ± 3%	11 ± 2%
Tricon-jugated	–	19 ± 1%	11 ± 1%	–	23 ± 4%	–	19 ± 2%	–	18 ± 2%	12 ± 1%
Tetraconju-gated.	–	11 ± 1%	14 ± 1%	–	15 ± 2%	–	7 ± 1%	–	7 ± 1%	13 ± 2%
Higher-order conjugates (5–8)	–	–	66 ± 10%	–	–	–	–	–	–	32 ± 3%

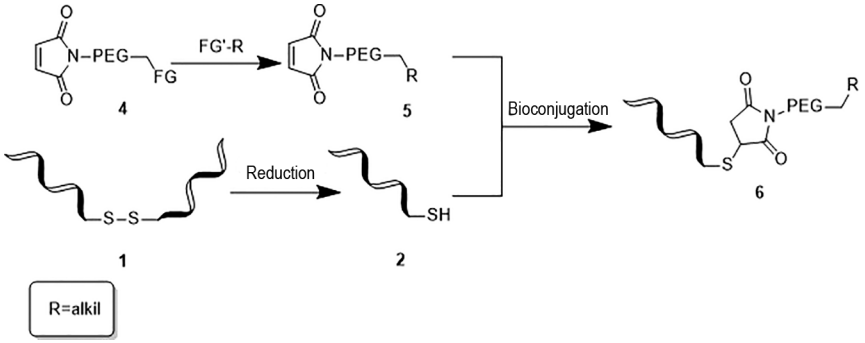

Fig. 10. **General scheme for the preparation of spidroin 6 modified with lipophilic chains.**

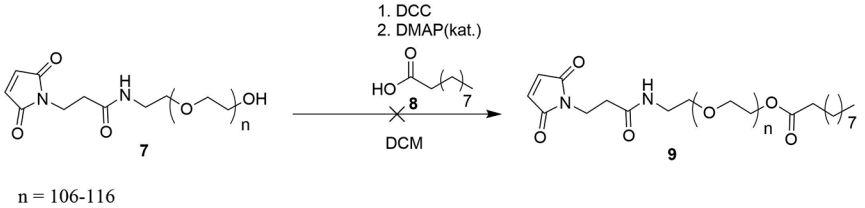

Fig. 11. **Conjugation of lipophilic carboxylic acids with Mal-PEG-OH.**

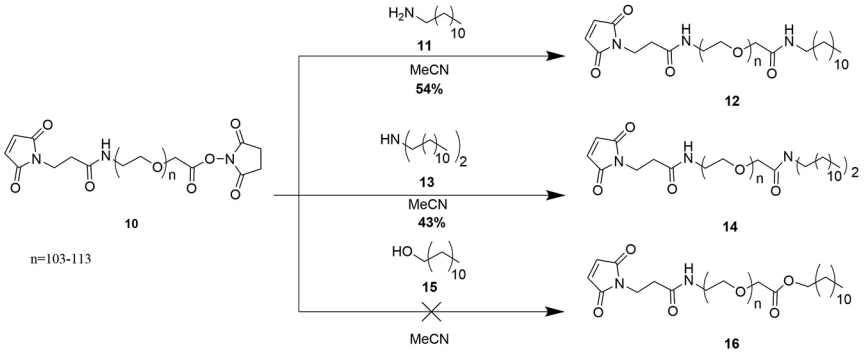

Fig. 12. **Conjugation of lipophilic moieties with 2-arm heterobifunctional PEG.**

In subsequent studies, we employed the activated NHS ester **10** (Mal-PEG-SCM). As in the previous case, conjugation with alcohols did not yield the desired product **16**, either under equimolar conditions or with an excess of reagent. A more successful approach proved to be the conjugation of **10** with aliphatic amines, which enabled the preparation of the desired products containing either one aliphatic chain **12** or two chains **14**.

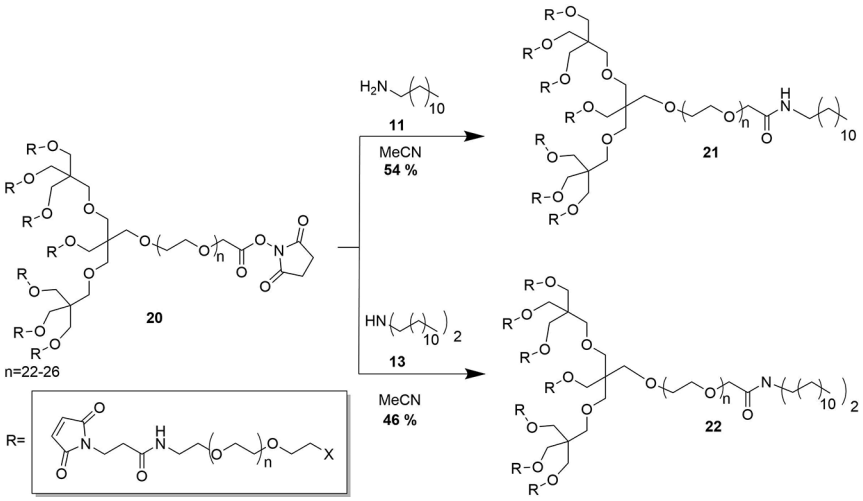

Fig. 13. **Conjugation of lipophilic moieties with 4-arm heterobifunctional PEG.**

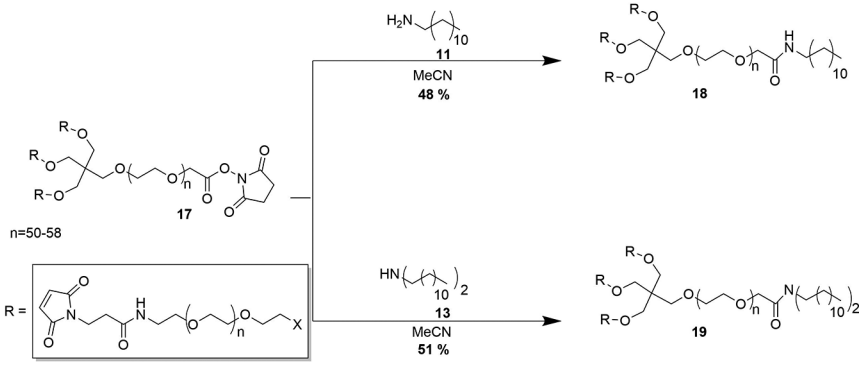

Fig. 14. **Conjugation of lipophilic moieties with 8-arm heterobifunctional PEG.**

Using multi-arm bifunctional PEGs **17** or **20**, this method also allowed the synthesis of four-arm PEG derivatives bearing one (compound **18**, 48% isolated yield) or two aliphatic chains (compound **19**, 51% isolated yield) (Fig. 13), as well as eight-arm PEG products **21** (54% isolated yield) and **22** (46% isolated yield) (Fig. 14).

It is important to maintain the correct stoichiometric ratio of starting materials: aliphatic amines should be used in only a slight excess relative to the PEG compound; otherwise, a side reaction occurs in which the amine undergoes an Aza–Michael reaction with the maleimide group. Precipitation of the product from a diethyl ether/DCM system allowed isolation of the desired compounds with an average yield of ~50% and with the maleimide double bond intact.

Table 2.3. **Bioconjugation Results with Lipophilic Groups**

	12 conjugate with F2F	**14 conjugate with F2F**	**18 conjugate with F2F**	**19 conjugate with F2F**	**21 conjugate with F2F**	**22 conjugate with F2F**
Unreacted protein	24%	22%	23 ± 6%	24 ± 6%	14 ± 3%	12 ± 5%
Monoconjugated	76%	78%	19 ± 1%	22 ± 4%	13 ± 4%	17 ± 3%
Diconjugated	–	–	35 ± 4%	26 ± 8%	14 ± 3%	8 ± 3%
Triconjugated	–	–	24 ± 2%	28 ± 9%	12 ± 3%	17 ± 5%
Higher-order conjugates (4–7)	–	–	–	–	47 ± 15%	46 ± 13%

The obtained compounds were subsequently conjugated with minispidroins using the optimized method; the results are summarized in Table 2.3. From these data, it can be seen that the overall substitution level and conjugation efficiency were relatively high, with most compounds yielding fully substituted products.

3. Spinning of Bioconjugates

In the silk glands, spider silk is formed through a sequence of processes. First, spidroins are synthesized in the tail region. In the ampullate sac, these proteins assemble into micelles with diameters of several tens of nanometers. At this stage, the protein concentration is extremely high – up to 50% w/v. [22] The micelles are then transported into the duct, where they become aligned and oriented along the channel axis. During this process, the pH of the environment decreases from 7.5 to 5.0, ion exchange occurs, and the spidroins undergo further concentration. Near the end of the duct, both acidity and protein concentration reach their maximum, and the proteins exist in a liquid-crystalline state. Finally, at the conical end of the duct, silk is spun as the fiber-forming proteins adopt a stable secondary helical structure.

Biomimetic spider silk spinning in the laboratory aims, as far as possible, to replicate the natural spinning process occurring in the gland. During spinning, changes in pH trigger molecular assembly. Unlike traditional methods that rely on harsh organic solvents, biomimetic spinning is based solely on aqueous buffers and mild conditions, thereby preserving the native structure and functionality of the proteins.[24]

To obtain fiber diameters closely resembling natural spider silk (2–4 μm), the fibers must be drawn through a long, narrow, funnel-shaped channel. This can be achieved using a specially prepared glass capillary with an internal diameter of 40–60 μm. Diameters below 40 μm lead to frequent clogging, rendering the capillary unusable. These glass capillaries were prepared with the assistance of OSI glassblower Gundars Leitis. The capillaries were fabricated from glass

pipettes by heating them in a flame and drawing them out. In the next step, the cooled capillary was broken under a microscope at the point where its diameter reached 40–60 μm.

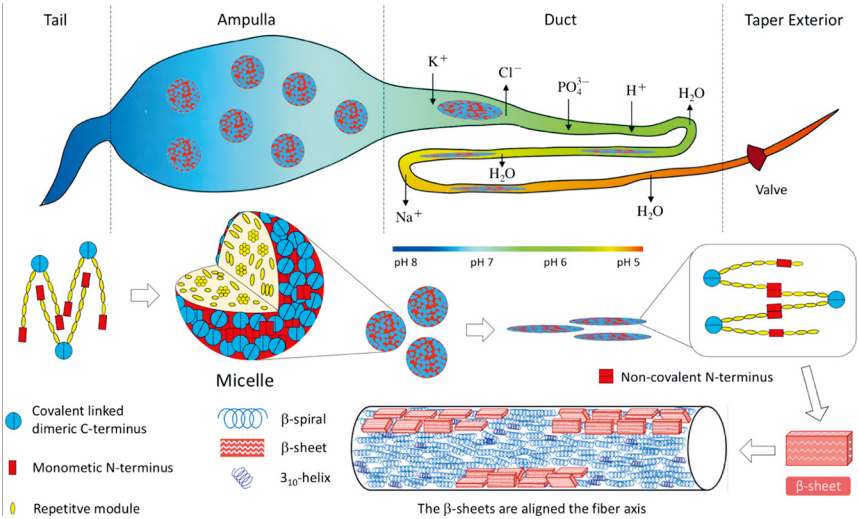

Fig. 15. **Schematic representation of the spider gland and spidroins. [23]**

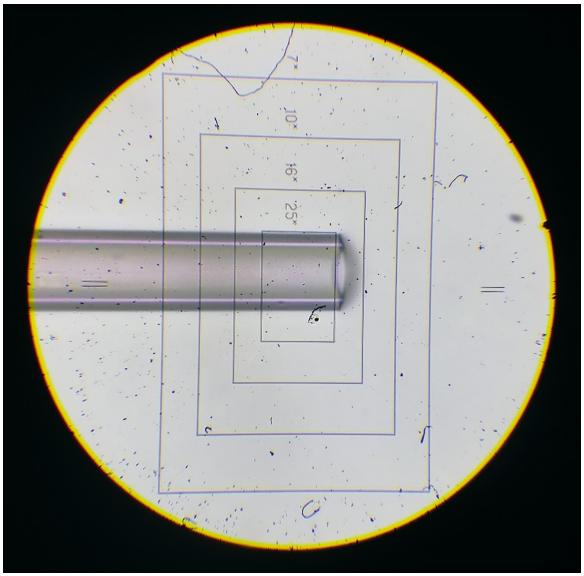

Fig. 16. **Glass capillary under the microscope after breaking.**

The spinning process itself is shown in Fig. 17. First, the protein is concentrated to ~150–300 mg/mL and injected through the previously described glass capillary into an acetate buffer with pH ~5. Experimentally, we determined that at lower protein concentrations fiber formation does not occur. The pH shift from 7.4 to ~5 induces instantaneous protein coagulation in the form of a filament, which is subsequently collected on a rotating frame. [24] The rotation speed of the collection frame was adjusted individually for each fiber in order to maximize stretching before collection, while minimizing fiber breakage. Increasing the distance between the capillary outlet and the collection frame enabled more effective fiber stretching, but at the cost of a higher risk of fiber rupture during the process.

In total, 14 different fibers were spun, of which 7 were various MaSp spidroin conjugates, 6 were F2F minispidroin conjugates, and one was non-conjugated F2F spidroin (Table 3.1).

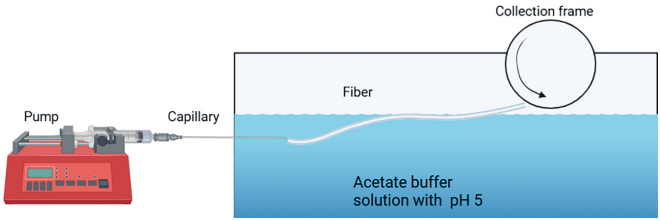

Fig. 17. **Schematic representation of the silk spinning apparatus.**

Table 3.1. **Efficiency of Bioconjugate Spinning**

No.	Minispidroin	Bioconjugated protein	Fiber spinning efficiency
1.	F2M	2-arm-PEG	–
2.	F2M	2- arm -PEG-C12	–
3.	F2M	2- arm -PEG-$(C12)_2$	–
4.	F2M	4- arm -PEG	+
5.	F2M	4- arm -PEG-C12	–
6.	F2M	4- arm -PEG-$(C12)_2$	–
7.	F2M	8- arm -PEG	–
8.	F2F	–	+++
9.	F2F	2- arm -PEG	+++
10.	F2F	4- arm -PEG	+++
11.	F2F	4- arm -PEG-C12	++
12.	F2F	4- arm -PEG-$(C12)_2$	+
13.	F2F	8- arm -PEG	+++
14.	F2F	8- arm -PEG-C12	–

+++ high spinning efficiency; the entire fiber was collected on the frame without a single break;
++ medium spinning efficiency; the fiber was fully collected on the frame but broke a few times;
+ low spinning efficiency; the fiber broke repeatedly during collection;
– spinning failed; no fiber could be obtained.

F4M and F6M conjugates were not used in spinning experiments due to their instability. These proteins proved to be sensitive to temperature fluctuations and were significantly less stable compared to F2M. Within only a few hours after purification, they precipitated, making preparation of spinning material impossible.

When spinning F2M bioconjugates, the obtained fibers were gel-like and broke upon even slight contact. Only one of the conjugates could be spun successfully, and this required a substantial reduction in spinning speed, collection frame distance, and rotation speed (Table 3.1, entries 1–7). The low spinning efficiency of F2M can be explained by the relatively small proportion of the repetitive domain in the protein, which leads to weaker intermolecular interactions.

In contrast, almost all samples containing F2F protein exhibited very good spinning efficiency (Table 3.1, entries 8–13). It was also observed that increasing the proportion of the lipophilic moiety in the bioconjugate reduced spinning efficiency (Table 3.1, entries 11, 12, and 14).

4. Physical Properties of the Obtained Fibers

The physical properties of the obtained fibers were tested in the laboratory of our collaborators in Sweden (A. Rising and B. Schmuck, Karolinska Institute). The tests were carried out at relatively low humidity (<30%), which is important because fully dried fibers exhibit poorer physical properties. The diameter of F2M 4-arm PEG fibers was among the largest (23–45 μm on average) (Fig. 18), which can be explained by the reduced spinning speed and the shorter distance between the capillary outlet and the collection frame. The variation in fiber diameter can likewise be attributed to frequent fiber breakage, which prevented uniform post-spinning stretching. These fibers showed minimal extensibility (Fig. 19). The tensile strength of these fibers (Fig. 20) was comparable to that of minispidroin fibers containing 12–20 repetitive domains. [25, 26] PEG nav manāmas ietekmes uz šķiedras izstiepjamību, PEG itself did not exhibit a noticeable effect on fiber extensibility when compared with other artificial fibers based on MaSp spidroin.

The extensibility (Fig. 19) and tensile strength (Fig. 20) of F2F 2-arm and 4-arm PEG fibers were similar to those of F2M 4-arm PEG. In contrast, both non-conjugated F2F and F2F 8-arm PEG fibers showed almost twice the tensile strength of the other samples, as well as 3–4 times higher strength compared to similar artificially spun fibers based on FlSp protein.[27]

The best results in fiber strain at break were observed for the F2F 8-arm PEG conjugate, which can be explained both by its high bioconjugation efficiency and its complex cross-linked structure.

Unfortunately, the introduction of lipophilic chains into the bioconjugates did not result in noticeable improvements in the physical properties of the fibers. The strain at break of F2F 4-arm PEG-C12 was higher compared with F2F 4-arm PEG; however, its stress at break was reduced. The bioconjugate containing two lipophilic side chains exhibited even lower mechanical properties.

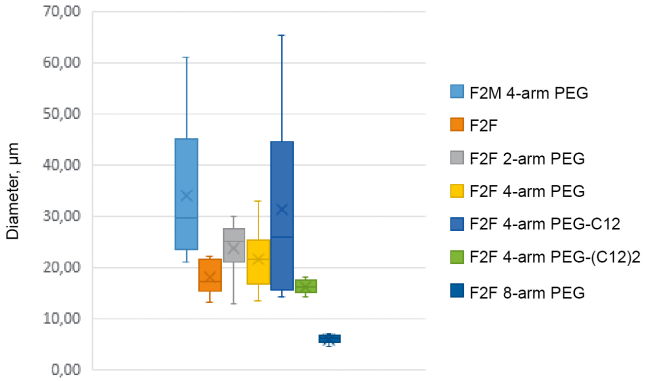

Fig. 18. **Average Diameter of Spun Fibers.**

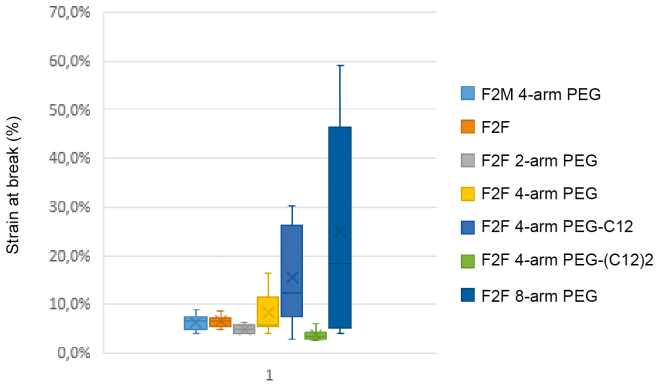

Fig. 19. **Strain at break (excluding gross errors).**

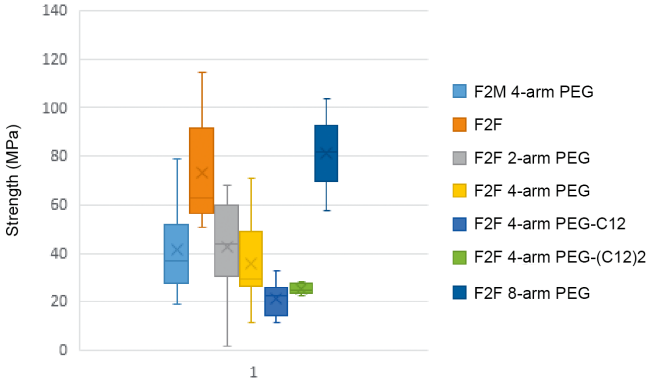

Fig. 20. **Stress at break (excluding gross errors).**

This indirectly suggests that the relative mass fraction of introduced lipophilic layers in the conjugate is too low to effectively protect the fiber from drying. For comparison, in natural spider silk the lipophilic layer accounts for ~3–5% of the fiber mass, whereas in our method the lipid fraction was only ~0.1%. [28]

In addition, F2F–PEG conjugates were studied using scanning electron microscopy (SEM) to compare fiber surface morphologies. These studies were carried out in collaboration with Prof. S. Gaidukov (RTU, Faculty of Materials Science and Applied Chemistry). It was found that all bioconjugate fibers exhibited spherical agglomerates on their surfaces. F2F 2-arm PEG (Fig. 22), F2F 4-arm PEG–C12 (Fig. 24), and F2F 8-arm PEG (Fig. 26) displayed similar surface morphologies, containing only a small number of spherical features. It was observed that a higher number of PEG arms increased the abundance of spherical structures on the fiber surface.

In the F2F 4-arm PEG sample (Fig. 23), the number of surface features increased drastically; a similar effect was seen in F2F 4-arm PEG–2C12 (Fig. 25). Moreover, the morphology of these features changed from spherical to irregular. By contrast, fibers obtained from non-conjugated F2F minispidroin (Fig. 21) showed smooth surfaces, indicating that the spherical structures observed on conjugated fibers are composed primarily of PEG and aliphatic chains.

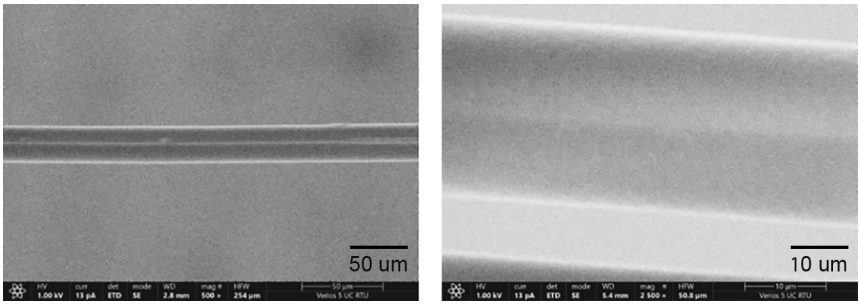

Fig. 21. **Surface morphology of F2F protein fibers.**

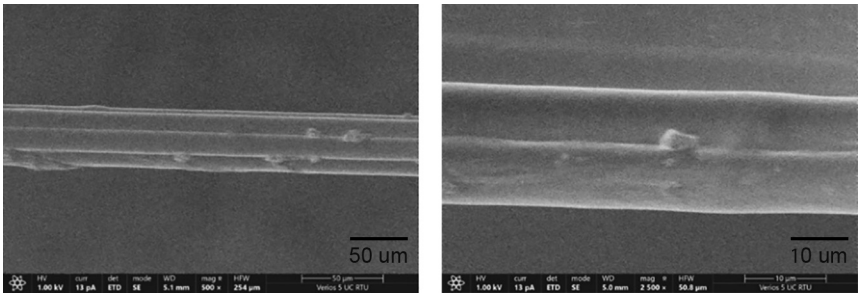

Fig. 22. **Surface morphology of F2F 2-arm PEG conjugate fibers.**

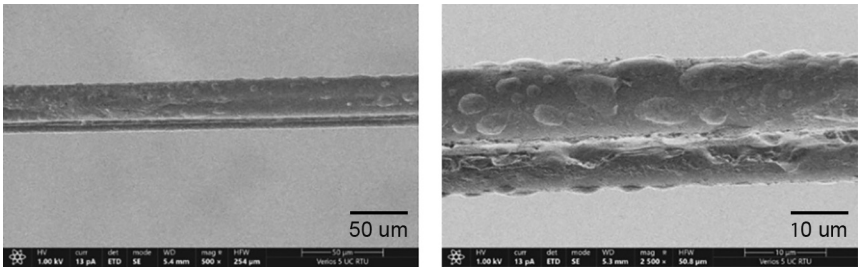

Fig. 23. **Surface morphology of F2F 4-arm PEG conjugate fibers.**

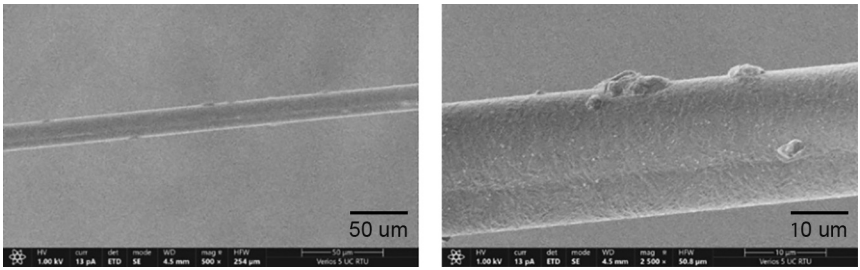

Fig. 24. **Surface morphology of F2F 4-arm PEG–C12 conjugate fibers.**

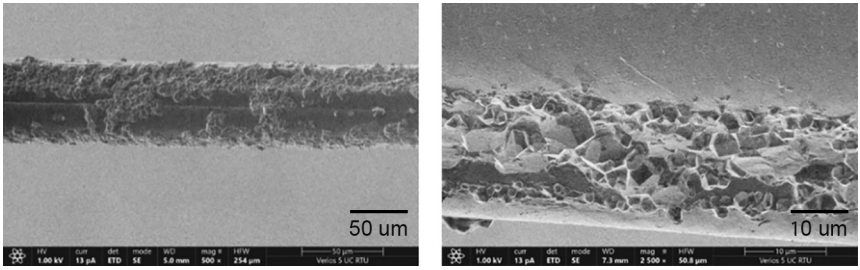

Fig. 25. **Surface morphology of F2F 4-arm PEG–2C12 conjugate fibers.**

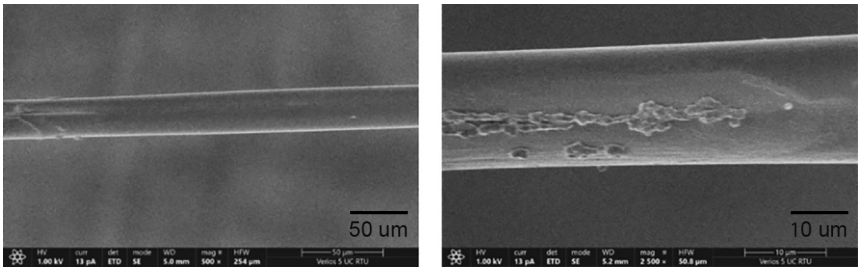

Fig. 26. **Surface morphology of F2F 8-arm PEG conjugate fibers.**

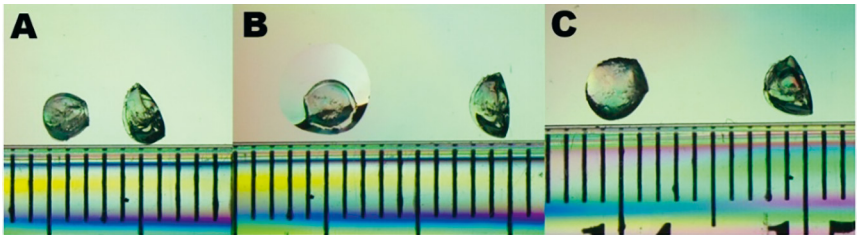

Fig. 27. **Two samples of bioconjugated spidroin.** Scale bar: 1 mm per division. A- both samples dried. B – one sample after the addition of deionized water. C – swollen sample (left) compared with dried sample.

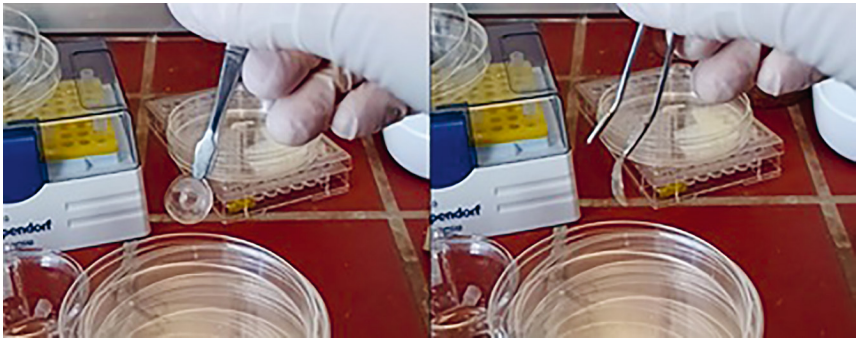

Fig. 28. **Spidroin-Based Lens-Shaped Material.**

In addition to spun fibers, the properties of the pre-spinning material were also examined. A dry protein bioconjugate was immersed in distilled water, and its swelling was observed.

These beads were initially relatively soft and elastic, but upon drying they shrank to about half their size and their shape became irregular (Fig. 27A). After the addition of water, we observed gradual diffusion of water through the sample walls (Fig. 27B). After 2 hours, the sample to which water had been added was dried and its diameter measured again (Fig. 27C). The sample had regained its previous spherical shape, its surface had become smoother, and its diameter increased from ~2 mm to ~4 mm, i.e., nearly twofold.

By optimizing the polymerization conditions of spidroin solutions, it was eventually possible to obtain a robust lens-shaped material with a diameter of ~20 mm and thickness of ~2 mm.

CONCLUSIONS

1. Complete reduction of the minispidroins used in this work requires 24 h at 4 °C with 10 equivalents of TCEP. Longer reduction times, higher temperatures, or larger reagent excesses lead to protein degradation.
2. The most effective method for removing TCEP from the reaction mixture is ion-exchange chromatography.
3. A 0.1–0.2 equivalent excess of protein relative to PEG–maleimide groups improves reaction efficiency.
4. For PEG conjugation with lipophilic moieties, a 0.05–0.1 equivalent excess of the lipophilic component should be used, and the reaction time should not exceed 1 h to avoid the undesired aza–Michael side reaction.
5. MaSp proteins are expressed at approximately twice the yield per liter of medium compared with FlSp.
6. FlSp bioconjugates exhibit significantly fewer breaks during spinning compared to MaSp.
7. Increasing the proportion of lipophilic groups in the bioconjugate decreases spinning efficiency.
8. Incorporation of PEG into the bioconjugate improves fiber strength, making it comparable to minispidroins containing 12–20 repetitive domains.
9. PEG does not negatively affect fiber strain at break compared with other artificial MaSp-based minispidroin fibers.
10. Reducing fiber diameter improves their mechanical properties.
11. The tensile strength of non-conjugated recombinant F2F minispidroin and the F2F 8-arm PEG conjugate is markedly higher than that of previously spun FlSp-based fibers.
12. Introduction of lipophilic groups did not significantly improve fiber physical properties. This can be explained by the much lower fraction of lipophilic components in the bioconjugates compared with natural spider silk.
13. The bioreactor allowed production of nearly 37 times more protein compared with flask cultivation.

REFERENCES

[1] Eisoldt, L., A. Smith, and T. Scheibel, *Decoding the secrets of spider silk.* Materials Today, 2011. **14**(3): pp. 80–86.

[2] *Spider Silk Market Size, Share & Trends Analysis Report by Technology (Genetically Modified E-Coil Fermentation, Genetically Modified Silkworm, Genetically Modified Yeast Fermentation) And Application (Automotive, Defense, Healthcare, Textile)- Market Outlook And Industry Analysis 2024–2031.* 2024; Available from: https://www.insightaceanalytic.com/report/spider-silk-market/1587.

[3] Venkatesan, H., J. Chen, and J. Hu, *Fibers Made of Recombinant Spidroins – A Brief Review.* AATCC Journal of Research, 2019. **6**(1_suppl): p.p 37–40.

[4] Fahnestock, S. R. and L.A. Bedzyk, *Production of synthetic spider dragline silk protein in Pichia pastoris.* Appl Microbiol Biotechnol, 1997. **47**(1): pp. 33–9.

[5] Schillberg, S., et al., *Critical Analysis of the Commercial Potential of Plants for the Production of Recombinant Proteins.* Front Plant Sci, 2019. **10**: p. 720.

[6] Copeland, C. G., et al., *Development of a Process for the Spinning of Synthetic Spider Silk.* ACS Biomater Sci Eng, 2015. **1**(7): p. 577–584.

[7] Xu, H. T., et al., *Construct synthetic gene encoding artificial spider dragline silk protein and its expression in milk of transgenic mice.* Anim Biotechnol, 2007. **18**(1): pp. 1–12.

[8] Whittall, D. R., et al., *Host Systems for the Production of Recombinant Spider Silk.* Trends in Biotechnology, 2021. **39**(6): pp. 560–573.

[9] Matthew, S. A. L. and F. P. Seib, *The Dawning Era of Anticancer Nanomedicines: From First Principles to Application of Silk Nanoparticles.* Advanced Therapeutics, 2025. **8**(1): p. 2400130.

[10] Dunn, A.L., S.P. Ahuja, and E.S. Mullins, *Real-world experience with use of Antihemophilic Factor (Recombinant), PEGylated for prophylaxis in severe haemophilia A.* Haemophilia, 2018. **24**(3): pp. e84–e92.

[11] Goel, N. and S. Stephens, *Certolizumab pegol.* MAbs, 2010. **2**(2): pp. 137–47.

[12] *Polymer-Protein Conjugates: From Pegylation and Beyond.* 1 ed. 2019, Amsterdam: Elsevier. 512.

[13] Jia, Q., R. Wen, and Q. Meng, *Novel Highly Soluble Chimeric Recombinant Spidroins with High Yield.* Int J Mol Sci, 2020. **21**(18).

[14] Connor, A., et al., *Novel insights into construct toxicity, strain optimization, and primary sequence design for producing recombinant silk fibroin and elastin-like peptide in E. coli.* Metabolic Engineering Communications, 2023. **16**: p. e00219.

[15] Askarieh, G., et al., *Self-assembly of spider silk proteins is controlled by a pH-sensitive relay.* Nature, 2010. **465**(7295): pp. 236–238.

[16] Kronqvist, N., et al., *Sequential pH-driven dimerization and stabilization of the N-terminal domain enables rapid spider silk formation.* Nature Communications, 2014. **5**(1): p. 3254.

[17] Sarr, M., et al., *The dimerization mechanism of the N-terminal domain of spider silk proteins is conserved despite extensive sequence divergence.* Journal of Biological Chemistry, 2022. **298**(5): p. 101913.

[18] Huang, Y., et al., *Scale up of fermentation of recombinant Escherichia coli for efficient production of spider drag silk protein MaSp1s and its dimers.* Microb Cell Fact, 2025. **24**(1): p. 108.

[19] Li, X., et al., *Customized Flagelliform Spidroins Form Spider Silk-like Fibers at pH 8.0 with Outstanding Tensile Strength.* ACS Biomater Sci Eng, 2022. **8**(1): pp. 119–127.

[20] Schmuck, B., et al., *High-yield production of a super-soluble miniature spidroin for biomimetic high-performance materials.* Materials Today, 2021. **50**: pp. 16–23.

[21] da Silva, A. J., et al., *Non-conventional induction strategies for production of subunit swine erysipelas vaccine antigen in rE. coli fed-batch cultures.* SpringerPlus, 2013. **2**(1): p. 322.

[22] Kantner, T., B. Alkhawaja, and A.G. Watts, *In Situ Quenching of Trialkylphosphine Reducing Agents Using Water-Soluble PEG-Azides Improves Maleimide Conjugation to Proteins.* ACS Omega, 2017. **2**(9): pp. 5785–5791.

[23] Arndt, T., et al., *Spidroin N-terminal domain forms amyloid-like fibril based hydrogels and provides a protein immobilization platform.* Nature Communications, 2022. **13**(1): p. 4695.

[24] Zhao, Y., et al., *Observation of spider silk by femtosecond pulse laser second harmonic generation microscopy.* Surface and Interface Analysis, 2019. **51**(1): pp. 56–60.

[25] Andersson, M., et al., *Biomimetic spinning of artificial spider silk from a chimeric minispidroin.* Nature Chemical Biology, 2017. **13**(3): pp. 262–264.

[26] Heidebrecht, A., et al., *Biomimetic Fibers Made of Recombinant Spidroins with the Same Toughness as Natural Spider Silk.* Advanced Materials, 2015. **27**(13): pp. 2189–2194.

[27] Teulé, F., et al., *Modifications of spider silk sequences in an attempt to control the mechanical properties of the synthetic fibers.* Journal of Materials Science, 2007. **42**(21): pp. 8974–8985.

[28] Adrianos, S. L., et al., *Nephila clavipes Flagelliform Silk-Like GGX Motifs Contribute to Extensibility and Spacer Motifs Contribute to Strength in Synthetic Spider Silk Fibers.* Biomacromolecules, 2013. **14**(6): pp. 1751–1760.

[29] Sponner, A., et al., *Composition and hierarchical organisation of a spider silk.* PLoS One, 2007. **2**(10): p. e998.